

Quartz cementation inhibited by crestal oil charge: Miller deep water sandstone, UK North Sea

A. M. E. MARCHAND^{1,2,*}, R. S. HASZELDINE², C. I. MACAULAY²,
R. SWENNEN¹ AND A. E. FALLICK³

¹*Fysico-Chemische Geologie, K.U. Leuven, Celestijnenlaan 200C, B-3001 Heverlee, Belgium,* ²*Department of Geology and Geophysics, The University of Edinburgh, Grant Institute, West Mains Road, Edinburgh EH9 3JW, UK,* and ³*Scottish Universities Research and Reactor Centre, Isotope Geosciences Unit, East-Kilbride, G75 0QF, UK*

(Received 15 June 1998; revised 11 February 1999)

ABSTRACT: In the Miller Field, diagenetic quartz abundance, isotopic compositions and salinities of quartz-cementing fluids display a distinct pattern which is related to the structural depth of the reservoir sandstones. Quartz cement volumes increase from the crest of the field (average $6.0 \pm 1.5\%$) towards the flanks of the field (average $13.2 \pm 2.1\%$) and directly reduce reservoir porosity. By integrating petrographic observations with results of fluid inclusion measurements and O isotope analyses of diagenetic quartz, the pattern of quartz cementation is seen to be related to the reservoir filling history. Oil filled the crest of the reservoir first and prevented extensive quartz cementation. At greater depth in the reservoir oil zone, quartz overgrowths continued to precipitate until inhibited by the developing oil column. Oxygen isotope compositions of diagenetic quartz imply that quartz cement continued to precipitate in the water zone of the reservoir up to the present day.

KEYWORDS: quartz cementation, Miller deep water sandstone, North Sea, diagenetic quartz.

The Miller Field is located along the fault-bounded western margin of the South Viking Graben in blocks 16/7b and 16/8b. The reservoir sequence comprises Upper Jurassic sandstones of the Brae Formation, which were deposited as a mid-fan channelized lobe. To the west of the Miller Field, the South Brae Field comprises the proximal slope apron channels of the fan system (Turner *et al.*, 1987). The South Brae and Miller fan deposits form part of an extensive syn-rift play in the North Sea. Near the graben edge in the South Brae Field, the Brae Formation sandstones consist of thick units of mud and sand-supported conglomerates and coarse grained sandstones. Further eastwards in the Miller

Field, these sandstones prograde into medium- to fine-grained more distal deposits. In the crest of the Miller Field, the Brae Formation occurs at a depth of 3970 m TVDSS, with the oil-water contact (OWC) at 4090 m TVDSS (Garland, 1993). The Kimmeridge Clay Formation, which laterally interfingers with the Brae Formation sandstones and also directly overlies the main reservoir, provides the source for the hydrocarbons (Rooksby, 1991).

As is the case in many North Sea clastic reservoirs, quartz cementation is a major cause of porosity loss in the Brae Formation sandstones in the Miller Field. The aim of this paper is to assess the formation conditions of the quartz cement and to discuss the implications of quartz precipitation for the distribution of porosity. In the crest of the field, porosity can be as high as 23% (Fig. 2a). This is higher than the 8% normally expected at depths

* E-mail: ann.marchand@glg.ed.ac.uk

>3.9 km, when the average North Sea sandstone porosity-loss gradient is ~8% per km depth (Emery *et al.*, 1993). In the deeper more cemented parts of the reservoir, the average porosity is ~13% (Rooksby, 1991).

We have carried out a systematic petrographic examination of the variations in quartz overgrowth abundance and corresponding porosity loss, and secondary porosity generation, between wells and at different depths. Quartz cement precipitation conditions were constrained by integrating fluid inclusion temperature data with O isotope geochemistry.

GEOLOGICAL AND STRUCTURAL SETTING

The Miller Field covers an area of 45 km² defined by a combination of structural and stratigraphic trapping (Rooksby, 1991). The Brae Formation has been subdivided chronostratigraphically into three units in the South Brae-Miller area. In the South Brae Field the basal Unit 3 is composed mainly of coarse-grained, proximal fan sediments which thin towards Miller, where Unit 3 is represented by thin sandstones interbedded with mudstones (Garland, 1993). Unit 2 is composed of sandstones and conglomerates in South Brae, but thickens and becomes finer grained eastwards towards the Miller area where it forms the main reservoir (Garland, 1993). The uppermost Unit 1 is present only in the north of the Miller Field where it is separated from Unit 2 by up to 50 m of Kimmeridge Clay Formation. According to Garland (1993) the distribution of Unit 1 emphasizes a change in the locus of sediment input to the north of the area, after the effective cessation of sand supply from the Southwest by the South Brae feeder channel. This study focuses mainly on the southern part of the Miller Field to ensure the sedimentological continuity of the submarine fan system from the South Brae to the Miller area. The southern part of the Miller Field has been thoroughly drilled and, based upon the depth of the top of the Brae Formation sandstones in several wells, a contour map was constructed (Fig. 1a). From this it is clear that the structure of the reservoir sandstone body forms an anticline. Different wells can be grouped according to their position in the anticline into crestal (top Brae Formation between 3970 and 4020 m TVDSS), mid-flank (top Brae Formation between 4020 and 4060 m TVDSS) and flank (top Brae Formation >4060 m TVDSS) wells.

METHODS

Blue epoxy-impregnated thin sections from wells 16/7b-A03 and 16/8b-3 (crest position), 16/7b-24 (mid-flank position) and 16/8b-5, 16/8b-A06 and 16/7b-26 (flank position) form the petrographic database for this study (Fig. 1a). Thin-sections were studied using a standard polarizing microscope, and the mineralogical composition was determined by standard point counting (500 counts/section). Authigenic quartz abundances were confirmed by combined scanning electron microscopy-cathodoluminescence (SEM-CL) and image analysis. Polished wafers for fluid inclusion analysis were made from samples from two crestal wells (16/8b-3 and 16/7b-A03), two wells from the mid-flank (16/7b-25 and 16/8b-A10) and three wells from the flank (16/7b-26, 16/8b-A06 and 16/7b-A11) (Fig. 1a). Microthermometric measurements on quartz overgrowths were performed using a Linkham heating-cooling stage THM600 equipped with a UV fluorescence analyser.

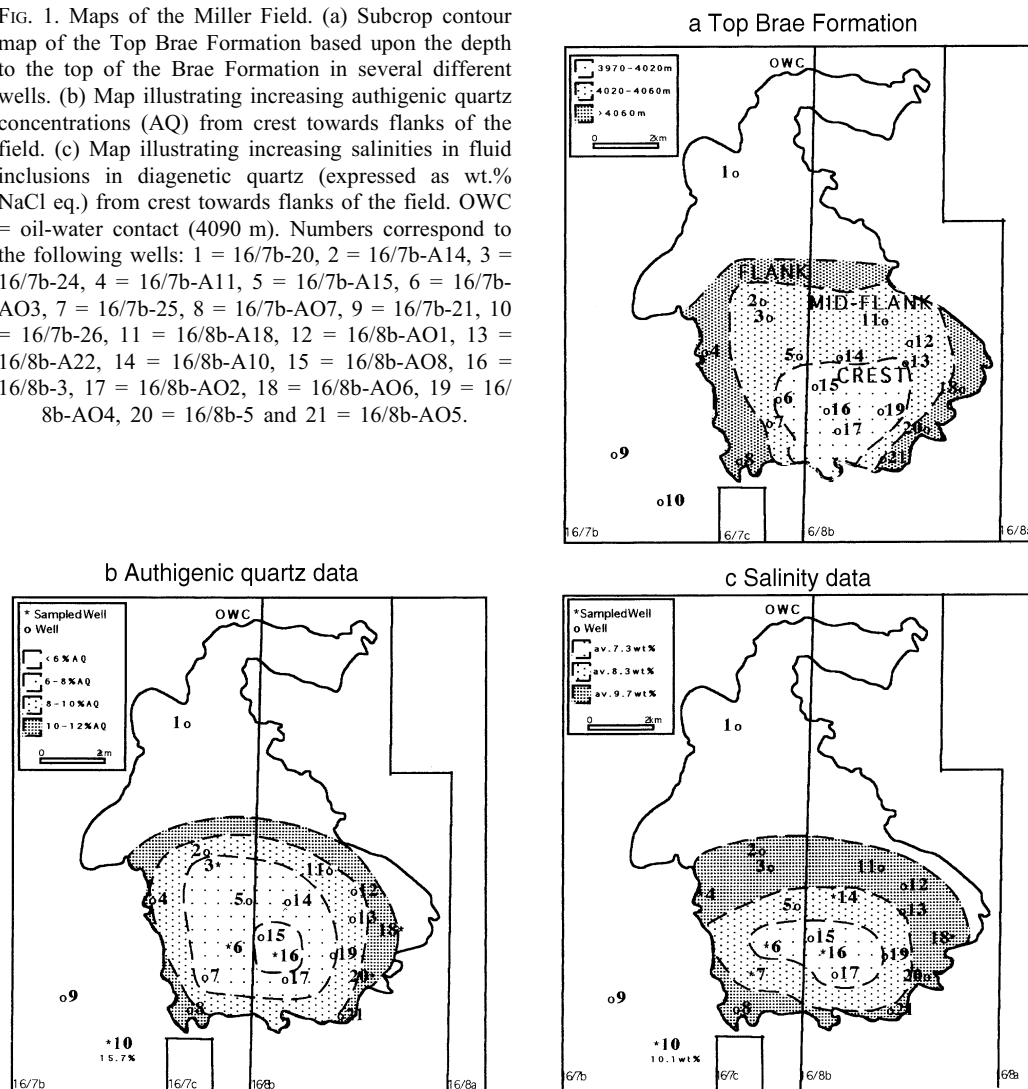
Stable O isotope analyses of authigenic quartz were carried out on samples from wells 16/8b-3 (crest), 16/7b-24 (mid-flank) and 16/8b-A06 (flank) (Fig. 1a). Samples from well 16/7b-20, located in the northern part of the field (Fig. 1a), were also included in the isotopic analyses. By using the procedure of Lee & Savin (1985), quartz overgrowths were separated from detrital quartz. Oxygen was extracted from four size-fractions from each sample (>85 µm, 85–53 µm, 53–30 µm and <30 µm) using a laser fluorination system based on that of Sharp (1990). The extracted O was subsequently converted to CO₂ and analysed on a VG PRISM III mass spectrometer. Purity checks using SEM-CL and image analysis showed that authigenic quartz was concentrated mainly in the finest size-fraction (Table 1a). Cross-plots of δ¹⁸O vs. authigenic quartz percentage in each size-fraction show good correlation and the δ¹⁸O value for quartz overgrowths was obtained by extrapolation towards 100% authigenic quartz. This analytical technique was described in Brint *et al.* (1991).

RESULTS

Petrography and diagenesis

Comparing the point-counted K-feldspar percentages with the scheme of McBride (1963), showed that the Brae Formation sandstones are subarkosic

FIG. 1. Maps of the Miller Field. (a) Subcrop contour map of the Top Brae Formation based upon the depth to the top of the Brae Formation in several different wells. (b) Map illustrating increasing authigenic quartz concentrations (AQ) from crest towards flanks of the field. (c) Map illustrating increasing salinities in fluid inclusions in diagenetic quartz (expressed as wt.% NaCl eq.) from crest towards flanks of the field. OWC = oil-water contact (4090 m). Numbers correspond to the following wells: 1 = 16/7b-20, 2 = 16/7b-A14, 3 = 16/7b-24, 4 = 16/7b-A11, 5 = 16/7b-A15, 6 = 16/7b-AO3, 7 = 16/7b-25, 8 = 16/7b-AO7, 9 = 16/7b-21, 10 = 16/7b-26, 11 = 16/8b-A18, 12 = 16/8b-AO1, 13 = 16/8b-A22, 14 = 16/8b-A10, 15 = 16/8b-AO8, 16 = 16/8b-3, 17 = 16/8b-AO2, 18 = 16/8b-AO6, 19 = 16/8b-AO4, 20 = 16/8b-5 and 21 = 16/8b-AO5.



in composition. Detrital quartz is the most abundant component comprising 60.3–87.1% of the detrital framework mineralogy. Feldspar is the second most abundant detrital component and comprises 4.7–16.5% of the bulk mineral composition. K-feldspar is the most common feldspar type present with minor amounts of plagioclase. Detrital clays, mica, pyrite and rock fragments all occur in trace amounts.

The first diagenetic mineral to precipitate after deposition of the sediments was concretionary calcite cement. Stable isotope analyses of the

calcite cement indicate that calcite precipitated from meteoric water during shallow burial (Table 1b). Similar calcite concretions in the Brae Formation sandstones were described and analysed by McLaughlin *et al.* (1994, 1996) in the adjacent South Brae Field.

Quartz cement concentrations in the Miller Field reservoir sandstones range from 3.2–16.8%. When authigenic quartz abundances are plotted against depth, and wells grouped together according to their position in the field, a distinct pattern emerges (Fig. 1b). Crestal wells display the lowest concen-

trations of overgrowths (average $6.0 \pm 1.5\%$), with increasing concentrations of quartz cement over the mid-flank (average $8.3 \pm 1.5\%$) to maxima in the flank wells (average $13.2 \pm 2.1\%$). From Fig. 2b, it becomes clear that authigenic quartz abundances increase towards the OWC. Below the OWC there is no particular trend in percentage of point-counted amounts of authigenic quartz with depth, but abundance is generally high.

Before, during and after quartz overgrowth precipitation, dissolution created considerable (4.6 up to 15.2%) amounts of secondary porosity. In the shallower parts of the field, secondary porosity exceeds primary depositional porosity in most samples (Fig. 2a). Partly dissolved K-feldspar grains and pores which outline feldspar grain shapes suggest that part of the secondary porosity resulted from feldspar dissolution.

Subsequent to secondary porosity formation, small amounts of pore-filling calcite, kaolinite, illite and some late stage cubic pyrite were precipitated.

Fluid inclusion analyses

Two types of inclusions were examined: primary aqueous liquid-vapour inclusions and petroleum inclusions. Inclusions located along detrital grain/overgrowth boundaries, and within overgrowths themselves, were analysed. Homogenization temperatures (T_h) were measured to determine minimum trapping temperatures at the time of quartz cementation. Because the samples are from a hydrocarbon reservoir, waters within the fluid inclusions are likely to be methane-bearing. Hence, it is reasonable to assume that homogenization temperatures are very similar to true trapping temperatures and do not require pressure correction (Hanor, 1980). Fluid inclusion ice melting temperatures were also determined to provide information about the salinity (expressed as NaCl wt.% equivalent) of the pore-fluids from which the quartz cements precipitated.

Data used in this study include both results of measurements carried out by Marchand and Macaulay, and data published in a Thermie programme report (1994). The T_h ranges from 82.9–125.8°C and salinities range from 5.1–11.8 wt.% NaCl eq. These data are not unusual and lie in the range reported from previous studies on authigenic quartz in clastic reservoirs in the North Sea (e.g. Saigal *et al.*, 1992; Walderhaug, 1994).

The T_h and salinities were plotted vs. depth, according to their structural position in the field (Fig. 3a,b). Homogenization temperatures display a wide range (min. 83°C and max. 126°C) of values in the crestal, shallower parts of the field (Fig. 3a). In the deeper mid-flank and flank wells, there is a trend of increasing homogenization temperatures with depth (Fig. 3a). Salinities display a slight increase in values over the whole depth range from crest to flank (Fig. 3b). Plotting the salinity data on a map of the field, a pattern similar (Fig. 1c) to that of authigenic quartz point-count abundance is observed. This pattern shows that less saline fluids were present in the shallower parts of the field, and denser, more saline fluids in the deeper parts. The present-day salinity trend (Fig. 3b) mirrors this pattern, indicating that salinity values have not changed significantly since quartz precipitation.

By examining the wafers under incident UV light on the microscope, petroleum-liquid dominant inclusions were detected. Hydrocarbon fluid inclusions trapped in quartz overgrowths indicate that oil emplacement occurred during quartz cementation (Walderhaug, 1990; Saigal *et al.*, 1992). According to Gluyas *et al.* (1993), variations in reservoir quality can occur because the crest of the reservoir received the earliest petroleum charge and protected the sandstones from extensive cementation. It is therefore plausible that the processes of quartz cementation and oil emplacement in the Miller field overlapped in time.

Oxygen isotope analysis

Values of extrapolated $\delta^{18}\text{O}$ of quartz overgrowths range between 16.5 and 24.0‰ and there is an increase in $\delta^{18}\text{O}$ with depth in wells 16/8b-3, 16/8b-AO6 and 16/7b-20 (Table 1a). Well 16/7b-24, on the contrary, displays a trend of decreasing $\delta^{18}\text{O}$ values with depth.

The extrapolated O isotope compositions of the quartz overgrowths are the result of the O isotope composition of the fluid from which quartz precipitated and of the temperature at which precipitation took place (Friedman & O'Neil, 1977). The isotopic composition of the quartz mineralizing fluid was calculated by combining the extrapolated $\delta^{18}\text{O}$ of the quartz overgrowths with homogenization temperatures measured in fluid inclusions. Since the extrapolated O isotope compositions represent an average $\delta^{18}\text{O}$ value measured over the whole overgrowth, calculations

TABLE 1. Results of O isotope analyses in authigenic quartz (a) and calcite cement (b) of samples from the Miller field. (a) Measured O isotope data, percentages of authigenic quartz (%AQ) in different size fractions and extrapolated O isotope values of authigenic quartz. Calculations of O isotope composition of porewaters were based upon the O isotope fractionation equation determined by Friedman & O'Neil (1977). (b) Calcite cement isotope data. The measured O isotope compositions in the calcite cement ($\delta^{18}\text{O}_{\text{SMOW calcite}}$) were used to calculate precipitation temperatures. Calculations were based upon the equation of Friedman & O'Neil (1977).

a		$\delta^{18}\text{O}_{\text{SMOW}}$ results (‰) in different size-fractions of quartz samples and % authigenic quartz in each size-fraction					Extrapolated $\delta^{18}\text{O}_{\text{SMOW}}$ (AQ) (‰)	T_h (average) (°C)	$\delta^{18}\text{O}_{\text{SMOW}}$ (pore-water) (‰)	
Position	Well	Depth (m TVDSS)	>85 μm $\delta^{18}\text{O}/\% \text{AQ}$	85–53 μm $\delta^{18}\text{O}/\% \text{AQ}$	53–30 μm $\delta^{18}\text{O}/\% \text{AQ}$	<30 μm $\delta^{18}\text{O}/\% \text{AQ}$				
crest	16/8b-3	3993.8	15.2/8.4	15.5/17.1	15.9/37.1	16.5/52.3	17.8	110.0	-2.3	
		4116.0	14.3/12.3	15.6/13.7	15.7/35.7	15.8/54.9	18.9	113.0	-0.9	
		4670.2	9.4/7.0	13.4/7.5	13.7/32.3	16.5/58.2	24.0	117.4	+4.7	
mid-flank	16/7b-24	4045.5	15.4/11.7	15.9/25.0	16.1/24.8	16.4/49.2	18.0	104.2	-2.9	
		4071.9	15.1/18.7	15.0/16.8	15.9/65.1	16.3/81.2	16.5	114.5	-3.1	
flank	16/8b-AO6	4074.8	14.9/14.6	15.4/21.3	15.8/47.3	16.0/72.8	16.8	111.9	-3.1	
		4084.3	15.2/10.7	15.8/23.0	16.2/49.7	16.1/62.5	17.1	108.5	-3.2	
	4121.1	14.7/14.1	15.8/23.7	15.8/33.0	16.2/52.8	19.0	108.5	-1.3		
	16/7b-20	4011.7	14.4/7.0	15.2/13.4	14.9/30.6	15.3/33.3	18.8	101.2	-2.4	
		4019.8	14.4/11.6	14.9/12.9	15.5/14.2	15.7/62.8	17.9	110.0	-2.2	
		4100.1	14.0/8.8	15.4/18.6	16.2/37.4	16.2/44.3	20.4	114.1	+0.7	
b		Well	Depth (m TVDSS)	$\delta^{18}\text{O}_{\text{SMOW}}$ calcite (‰)	$T_{\text{precipitation}}$ meteor. water (°C)	$T_{\text{precipitation}}$ mar. water (°C)	MCP (%)	S (%)	Calculated burial depth (km)	Calculated temperature (°C)
16/7b-28			4102.4	23.8	15.5	44.4	43.6	56.4	0.43	13.0
			4104.0	23.0	19.0	49.1	43.8	56.2	0.42	12.5
			4106.1	20.9	28.4	62.5	34.8	65.2	1.27	38.0
			4106.2	19.9	33.5	68.8				
16/8b-A10			4094.1	19.6	35.0	70.9	39.0	61.0	0.84	25.3
			4102.4	22.1	22.7	54.6	41.8	58.2	0.59	17.6
			4104.4	19.0	38.2	75.4	30.2	69.8	1.79	53.7
16/7b-24			4084.0	21.7	24.5	56.5				
			4084.1	16.9	49.7	93.5	33.6	66.4	1.40	41.9
			4084.7	16.7	50.9	93.5				
			4085.1	15.4	59.1	106.5	39.6	60.4	0.79	23.6
			4085.6	16.4	52.7	96.2	33.6	66.4	1.40	41.9
		4085.8	18.0	43.2	83.3	32.6	67.4	1.51	45.2	

Inhibition of quartz cementation, UK North Sea

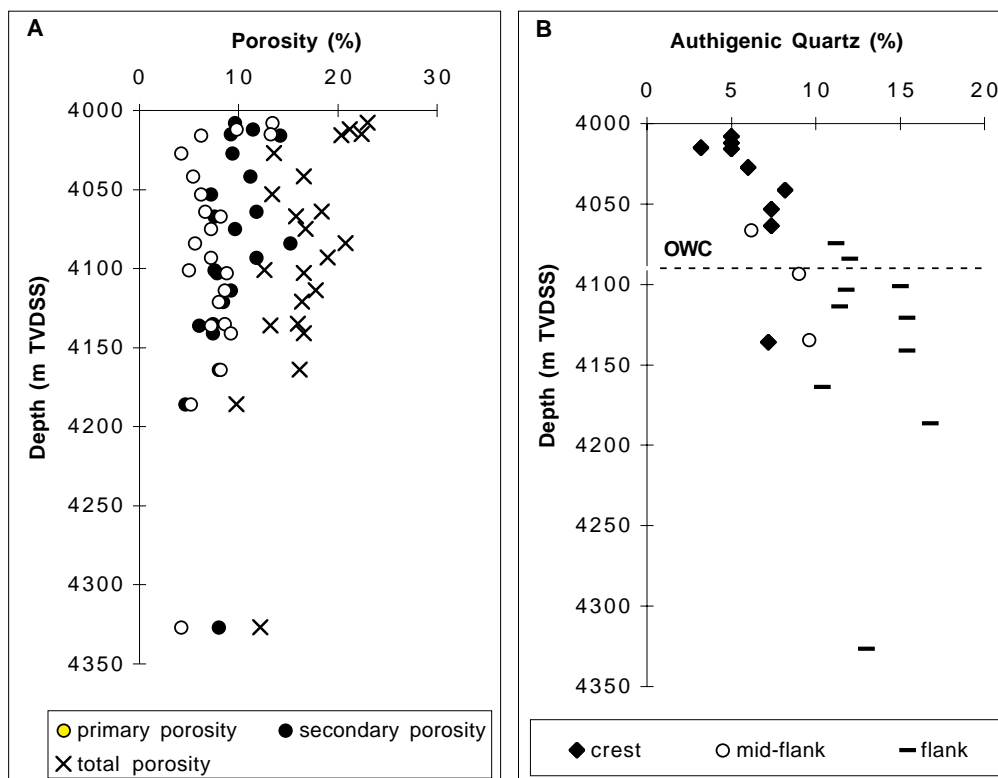


FIG. 2. Petrographic data. (a) Primary, secondary and total (primary + secondary) porosity variation with depth in the Brae Formation sandstones in the Miller field. (b) Authigenic quartz abundance data plotted against depth. Data are grouped according to the position of the well in the field, where crest = data from wells 16/8b-3 and 16/7b-AO3, mid-flank = data from well 16/7b-24 and flank = data from wells 16/7b-26, 16/8b-5 and 16/8b-AO6. All porosity and authigenic quartz abundance values are point-count values (500 counts/thin-section).

were carried out with the average T_h measured in the fluid inclusions in each sample (Table 1a). The pore-fluid isotopic compositions in the four wells, calculated by this method, range between -3.2 and $+4.7\%$. There is a different trend in O isotope compositions in the oil zone from that in the water zone (Fig. 3c). In the oil zone, calculated pore-water $\delta^{18}\text{O}$ compositions display a narrow range between -2.2 and -3.2% . In the water zone, calculated pore-water $\delta^{18}\text{O}$ compositions display a wider range of values between -1.3 and $+4.7\%$. Likely water types from which the quartz overgrowths could have precipitated in the Upper Jurassic sandstones are meteoric water, marine water or basinal water, with estimated $\delta^{18}\text{O}$ values respectively of -7% (Hamilton *et al.*, 1987; Hudson & Andrews, 1987), -1.2% (Shackleton &

Kennett, 1975) and $+2$ to $+5\%$ (Egeberg & Aagaard, 1989; Wilkinson *et al.*, 1992). According to Aplin *et al.* (1993) it is difficult to identify uniquely the origin of a formation water because mixtures can explain most of the compositional variations observed. Nevertheless, we feel that constraints can be placed on the origin of quartz-cementing fluids and these are discussed below.

DISCUSSION

Fluid interpretation

Results of O isotope analyses of authigenic quartz in the Miller Field show that fluids in the oil zone have an isotopically different composition compared to those calculated in the water zone

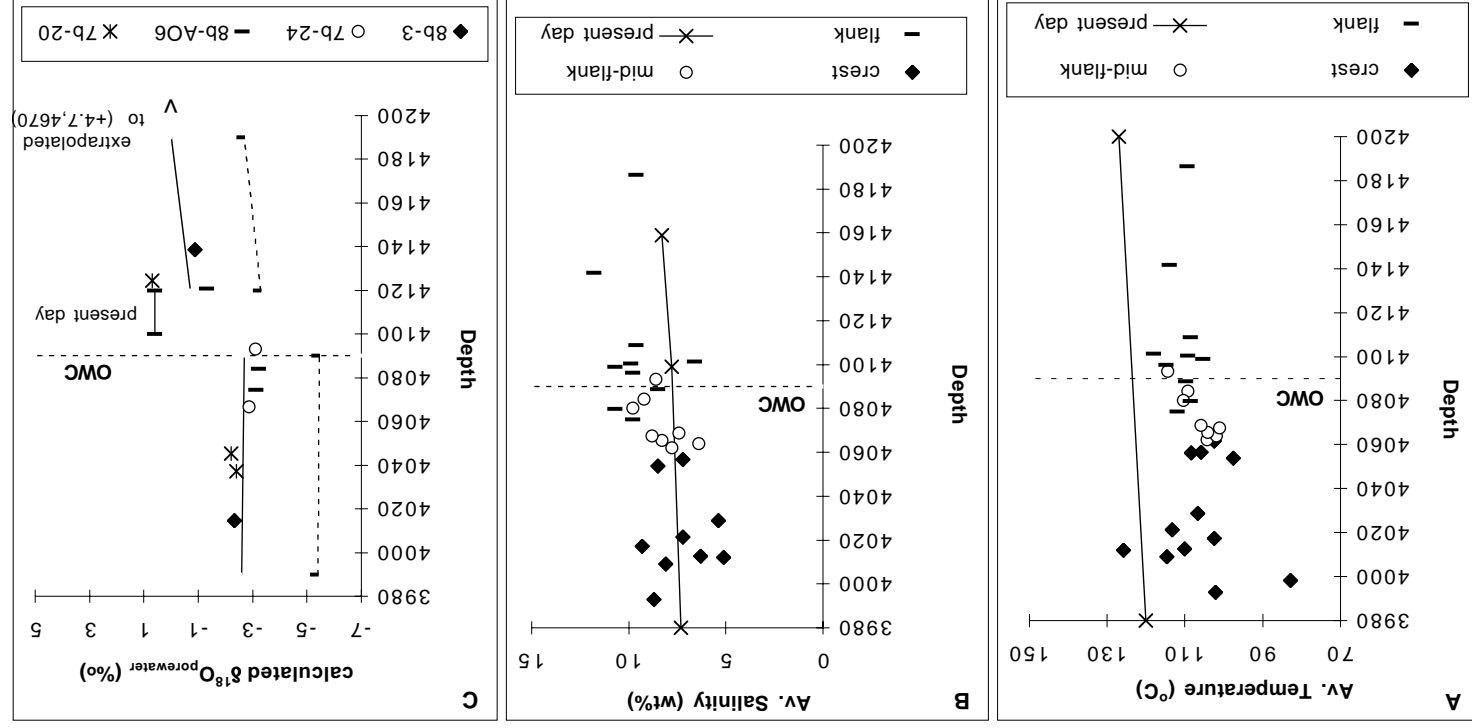


Fig. 3. Geochemical data. Average homogenization temperature (a) and average salinity (b) data versus depth. Data are grouped according to the position of the well in the field, where crest = data from wells 16/7b-AO3, mid-flank = data from wells 16/7b-25 and 16/8b-A10 and flank = data from wells 16/7b-26, 16/8b-AO6 and 16/8b-A11. Present-day temperatures are measured reservoir temperatures. Present day salinities of formation water were taken from Smalley and Warren (1994). (c) $\delta^{18}\text{O}$ variation with depth in different wells. Calculations of the pore-fluid isotopic composition were carried out by using the average homogenization temperatures measured in fluid inclusions in authigenic quartz of each sample. The solid lines represent the best fit lines through the data set. There is a different trend in oxygen isotope values in the oil zone from that in the water zone. Data point (+4.7, 4670) from well 16/8b-3 was not included in the cross-plot in order to allow a better overview of the bulk of the data set. The present-day O isotope value of formation water is indicated on the graph by a solid line. The present-day values were measured in 16/8b-5 and were taken from Smalley & Warren (1994). The dashed lines represent the best fit lines through the porewater isotope compositions calculated by using 20° lower than the average measured homogenization temperature in each sample. This dataset displays a similar trend to the solid lines but is shifted towards lower $\delta^{18}\text{O}$ values. OWC = oil-water contact (4090 m TVDSS).

(Fig. 3c). Fluid inclusion salinities display an increase of values with depth. Less saline fluids are present in the crest of the field, and more saline fluids at the flanks (Figs. 1c, 3b).

The calculated O isotopic compositions of pore-fluids in the oil zone display values ranging between -2.2 and -3.2‰ (Table 1a). This range in pore-fluid $\delta^{18}\text{O}$ values suggests a mixing of pore-water of isotopic composition similar to Upper Jurassic marine water (-1.2‰) with pore-water of isotopic composition similar to Upper Jurassic meteoric water (-7‰). The influence of marine water is feasible since the Brae Formation sandstones are marine deposits. Oxygen isotope data from early concretionary calcite cement in the Brae Formation sandstones in the Miller Field (Table 1b) attest to the presence of meteoric water in the reservoir during shallow burial. The recorded salinities (Figs. 1c, 3b) of the quartz cementing fluids in the oil zone are, however, greater than those of seawater (3.5 wt.% NaCl eq.) or fresh water (<0.5 wt.% NaCl eq.). Worden (1996) suggested that clastic and carbonate diagenesis may have an influence upon the overall salinity of formation waters. According to Worden (1996), the dissolution of K-feldspar and subsequent formation of kaolinite and quartz reduces the water volume and increases halogen concentrations proportionally. Since K-feldspar dissolution is observed throughout the reservoir sandstones, it may have contributed to elevated pore-water salinities.

From Fig. 3c it can be seen that fluids generally become more enriched in ^{18}O with depth. The deepest sample, at 4670 m TVDSS in well 16/8b-3, clearly displays the isotope signature of basinal waters (Table 1a). Enrichment in ^{18}O of formation waters is generally ascribed to reaction with clay minerals and carbonates (Clayton *et al.*, 1966; Suchecki & Land, 1983). During water-rock reactions at elevated temperatures, O isotopes are repartitioned between minerals and pore-water, resulting in a relative enrichment of water in ^{18}O .

As can be seen in Fig. 3c, the present day formation water is slightly more evolved compared to the calculated $\delta^{18}\text{O}$ values of pore-water in the water zone. This can be explained by a continued growth of quartz cement in the water zone up to the present day. Because the isotope compositions represent bulk overgrowth compositions, each time new precipitated quartz was added onto the overgrowth, the calculated pore-water composition will shift towards the $\delta^{18}\text{O}$ composition of the more

isotopically evolved formation waters present at that time in the water zone. In the oil zone, quartz growth was halted by oil charge into the reservoir. As a result, original compositions of pore-fluid from which quartz precipitated are preserved.

Some authors have advocated re-equilibration of fluid inclusions by leakage or stretching to present-day temperatures (Haszeldine & Osborne, 1993; Osborne & Haszeldine, 1993). Others state that resetting of fluid inclusions in quartz is rare under diagenetic conditions (e.g. Worden *et al.*, 1995). Since there is no conclusive evidence that the measured fluid inclusions were not reset, the isotopic compositions of pore-waters were also calculated using 20° lower than the average measured T_h in each sample. Results of such calculations are presented in Fig. 3c. It can be seen that the calculated pore-water compositions display a similar trend to calculated pore-water compositions calculated with average T_h , but shifted towards lower values. The re-calculated $\delta^{18}\text{O}$ pore-water compositions point towards a larger component of Upper Jurassic meteoric water (-7‰ ; Hamilton *et al.*, 1987; Hudson & Andrews, 1987). Given the mid-fan setting of the sandstones, this seems less likely than the pore-water compositions calculated by using average T_h values.

QUARTZ CEMENTATION MODEL

In the Miller Field, diagenetic quartz abundances increase with structural depth towards the OWC in the reservoir sandstones. In the water zone, diagenetic quartz abundance is high overall. Porosity distribution in the reservoir is opposite to the quartz cement distribution (Fig. 2). Maximum porosities occur in the crest of the field (up to 23%). A petrographic study of the reservoir sandstones showed that, particularly in the shallow parts of the reservoir, the contribution of secondary porosity to total porosity is high (Fig. 2a). The pattern of increasing quartz cement and decreasing porosities with depth is interpreted as being the result of oil charge into the reservoir. This concept of oil halting quartz growth and preserving porosity in the oil zone, is confirmed by the presence of petroleum fluid inclusions in the authigenic quartz and by different calculated pore-water $\delta^{18}\text{O}$ compositions in oil zone and water zone.

The overall rate of quartz cementation is related to silica source, silica transportation from the site of the source to the site of cementation, and quartz

cement precipitation (Worden *et al.*, 1998). When oil starts to accumulate in the crest of the anticlinal structure in the Miller Field, quartz cementation will initially slow down because of a decreased silica diffusion rate in the presence of oil (Worden *et al.*, 1998). Eventually, when oil saturations become sufficiently high, quartz cementation will be inhibited because the fluids dissolving and precipitating silica cannot gain access to the detrital quartz grains any more (Worden *et al.*, 1998). This results in low amounts of authigenic quartz in the crestal parts of the field and consequently higher preserved porosities. At greater depth in the reservoir, quartz cement will continue to precipitate until inhibited by the developing oil column. This explains the observed increase of quartz cement abundance and decrease of porosity with depth towards the present-day OWC in the reservoir. In the water zone, quartz cementation has continued up to the present, resulting in an overall high authigenic quartz abundance.

CONCLUSIONS

(1) In the Miller Field, diagenetic quartz abundances, O isotopic compositions and fluid inclusion salinities all display similar spatial patterns which are related to the structural depth of the reservoir sandstones.

(2) The observed quartz cement and porosity distributions in the reservoir are explained by progressive hydrocarbon filling of the anticlinal structure of the Miller Field. This resulted in low diagenetic quartz abundances and preserved porosities in the crestal parts of the anticline, and higher quartz cement abundances and lower porosities towards the OWC. In the water zone, quartz cementation continued unhindered up to the present day resulting in an overall high abundance of diagenetic quartz.

(3) Fluid inclusion salinities display similar values to present-day formation water salinity values. This indicates that the salinity of pore-fluids has not changed significantly since quartz precipitation. Petroleum fluid inclusions attest to the presence of oil during quartz cementation.

(4) In the oil zone, authigenic quartz precipitated from a mixing of pore-waters with O isotope compositions similar to Upper Jurassic marine and meteoric water. In the water zone, pore-water O isotope compositions become more enriched in ^{18}O as a result of water-rock reactions. Continued quartz

cementation in the water zone caused the calculated $\delta^{18}\text{O}$ pore-water values to shift towards the $\delta^{18}\text{O}$ composition of the more isotopically evolved formation waters present at that time in the water zone. Hence, the present-day $\delta^{18}\text{O}$ formation water composition is only slightly more evolved compared to calculated $\delta^{18}\text{O}$ values in the water zone.

ACKNOWLEDGMENTS

The authors gratefully acknowledge the DTI Core Store (Edinburgh) and BP for access to core material and Miller Field data. This research was carried out at Fysico-Chemische Geologie of the Katholieke Universiteit Leuven (Belgium) and at the Isotope Geosciences Unit of the Scottish Universities Environmental Research Centre (SUERC) in the framework of a grant provided by the Flemish government to stimulate international collaboration (VIS 95-4). The SUERC is supported by NERC and a consortium of Scottish Universities. The authors thank R. Worden and an anonymous reviewer for their constructive comments which helped to improve the manuscript. The authors' interpretations are not necessarily the views of BP.

REFERENCES

- Aplin A.C., Warren E.A., Grant S.M. & Robinson A.G. (1993) Mechanisms of quartz cementation in North Sea reservoir sandstones: constraints from fluid composition. Pp. 7–22 in: *Diagenesis and Basin Development* (A. Horbury & A. Robinson, editors). Amer. Assoc. Petrol. Geol. Stud. Geol., **36**.
- Baldwin B. & Butler C.O. (1985) Compaction curves. *Amer. Assoc. Petr. Geol. Bull.* **69**, 622–626.
- Brint J.F., Hamilton P.J., Haszeldine R.S., Fallick A.E. & Brown S. (1991) Oxygen isotope analysis of diagenetic quartz overgrowths from the Brent sands: A comparison of two preparation methods. *J. Sed. Pet.* **61**, 527–533.
- Clayton R.N., Friedman I., Graf D.L., Mayeda T.K., Meents W.F. & Shimp N.F. (1966) The origin of saline formation waters. *J. Geophys. Res.* **71**, 3869–3882.
- Egeberg P.K. & Aagaard P. (1989) Origin and evolution of formation waters from oil fields on the Norwegian shelf. *Appl. Geochem.* **4**, 131–142.
- Emery D., Smalley P.C. & Oxtoby N.H. (1993) Synchronous oil migration and cementation in sandstone reservoirs demonstrated by quantitative description of diagenesis. *Phil. Trans. R. Soc. London*, **344**, 115–125.
- Friedman I. & O'Neil J.R. (1977) Compilation of stable

- isotope fractionation factors of geochemical interest. In: *Data of Geochemistry, 6th edition* (M. Fleischer, editor). US Geol. Survey Prof. Paper, **440-kk**.
- Garland C.A. (1993) Miller Field: reservoir stratigraphy and its impact on development. Pp. 401–414 in: *Petroleum Geology of Northwest Europe: Proc. 4th Conf.* (J.R. Parker, editor). Geological Society, London.
- Gluyas J.G., Robinson A.G., Emery D., Grant S.M. & Oxtoby N.H. (1993) The link between petroleum emplacement and sandstone cementation. Pp. 1395–1402 in: *Petroleum Geology of Northwest Europe: Proc. 4th Conf.* (J.R. Parker, editor). Geological Society, London.
- Hamilton P.J., Fallick A.E., Macintyre R.M. & Elliott S. (1987) Isotopic tracing of the provenance and diagenesis of Lower Brent Group sands, North Sea. Pp. 939–949 in: *Petroleum Geology of Northwest Europe* (J. Brooks & K. Glennie, editors). Graham & Trotman, London.
- Hanor J.S. (1980) Dissolved methane in sedimentary brines: Potential effect on the PVT properties of fluid inclusions. *Econ. Geol.* **75**, 603–609.
- Haszeldine R.S. & Osborne M. (1993) Fluid inclusion temperatures in diagenetic quartz reset by burial: implications for oilfield cementation. Pp. 35–46 in: *Diagenesis and Basin Development* (A. Horbury & A. Robinson, editors). Amer. Assoc. Petrol. Geol. Stud. Geol. **36**.
- Hudson J.D. & Andrews J.E. (1987) The diagenesis of the Great Estuarine Group, Middle Jurassic, Inner Hebrides, Scotland. Pp 259–276 in: *Diagenesis of Sedimentary Sequences* (J.D. Marshall, editor). Blackwell, Oxford.
- Lee M. & Savin S.M. (1985) Isolation of diagenetic overgrowths on sand grains for oxygen isotope analysis. *Geochim. Cosmochim. Acta*, **49**, 497–501.
- McBride E.F. (1963) A classification of common sandstones. *J. Sed. Pet.* **33**, 664–669.
- McLaughlin O.M., Haszeldine R.S., Fallick A.E. & Rogers G. (1994) The case of the missing clay, aluminium loss and secondary porosity, South Brae oilfield, North Sea. *Clay Miner.* **29**, 651–663.
- McLaughlin O.M., Haszeldine R.S. & Fallick A.E. (1996) Quartz diagenesis in layered fluids in the South Brae oilfield, North Sea. *SEPM Spec. Publ.* **55**, 103–113.
- Osborne M. & Haszeldine R.S. (1993) Evidence for resetting of fluid inclusion temperatures from quartz cements in oilfield. *Marine Petrol. Geol.* **10**, 271–278.
- Rooksby S.K. (1991) The Miller Field, blocks 16/7b, 16/8b UK North Sea. Pp. 159–164 in: *United Kingdom Oil and Gas Fields, 25 years Commemorative vol.* (I.L. Abbotts, editor). Geological Society Memoir **14**.
- Saigal G.C., Bjorlykke K. & Larter S. (1992) The effects of oil emplacement on diagenetic processes – examples from the Fulmar reservoir sandstones, central North Sea. *Amer. Assoc. Petr. Geol. Bull.* **76**, 1024–1033.
- Shackleton N.J. & Kennett J.P. (1975) Paleotemperature history of the Cenozoic and the initiation of Antarctic glaciation: Oxygen and carbon analyses in DSDP sites 277, 279, 281. Pp. 653–659 in: *Initial Report DSDP 24* (J.P. Kennett & R.E. Howtz, editors), Washington.
- Sharp Z.D. (1990) A laser-based microanalytical method for the in-situ determination of oxygen isotope ratios in silicates and oxides. *Geochim. Cosmochim. Acta*, **54**, 1353–1357.
- Smalley P.C. & Warren E.A. (1994) The Miller Field. P. 52 in: *North Sea Formation Waters Atlas* (E.A. Warren & P.C. Smalley, editors). Geological Society London, Memoir **15**.
- Suchocki R.N. & Land L.S. (1983) Isotopic geochemistry of burial-metamorphosed volcanogenic sediments, Great Valley sequence, California. *Geochim. Cosmochim. Acta*, **47**, 1487–1499.
- Thermie (1994) Miller field demonstration. P. 42 in: *Thermie Reservoir Geochemistry Project report*. Newcastle Research Group in Fossil Fuels and Environmental Geochemistry (University of Newcastle, UK), BP Exploration (Sunbury-on-Thames, UK), Geolab Nor (Trondheim, Norway), Institut Francais du Petrole (France), Department of Geology (University of Manchester, UK).
- Turner C.C., Cohen J.M., Connell E.R. & Cooper D.M. (1987) A depositional model for the South Brae oilfield. Pp. 853–864 in: *Petroleum Geology of Northwest Europe* (J. Brooks & K. Glennie, editors). Graham & Trotman, London.
- Walderhaug O. (1990) A fluid inclusion study of quartz-cemented sandstones from offshore mid-Norway – possible evidence for continued quartz cementation during oil emplacement. *J. Sed. Pet.* **60**, 302–310.
- Walderhaug O. (1994) Temperatures of quartz cementation in Jurassic sandstones from the Norwegian continental shelf – evidence from fluid inclusions. *J. Sed. Res.* **A64**, 311–323.
- Wilkinson M., Crowley S.F. & Marshall J.D. (1992). Model for the evolution of oxygen isotope ratios in the porefluids of mudrocks during burial. *Marine Petrol. Geol.* **9**, 98–105.
- Worden R.H., Warren E.A., Smalley P.C., Primmer T.J. & Oxtoby N.H. (1995) Discussion of ‘Evidence for resetting of fluid inclusion temperatures from quartz cements in oilfields’ by Osborne and Haszeldine (1993). *Marine Petrol. Geol.* **12**, 566–570.
- Worden R.H. (1996). Controls on halogen concentrations in sedimentary formation waters. *Mineral. Mag.* **60**, 259–274.
- Worden R.H., Oxtoby N.H. & Smalley P.C. (1998). Can oil emplacement prevent quartz cementation in sandstones? *Petrol. Geosci.* **4**, 129–137.